Determining the Molecular Weight of Polyelectrolytes Using the Rouse Scaling Theory for Salt-free Semidilute Unentangled Solutions

Aijie Han¹, Veera Venkata Shravan Uppala², Daniele Parisi¹, Christy George³,

Benjamin J. Dixon¹, Camila Denise Ayala¹, Xiuli Li², Louis A. Madsen^{2*}, Ralph H. Colby^{1*}

¹Materials Science and Engineering and Materials Research Institute,

The Pennsylvania State University, University Park, PA 16802

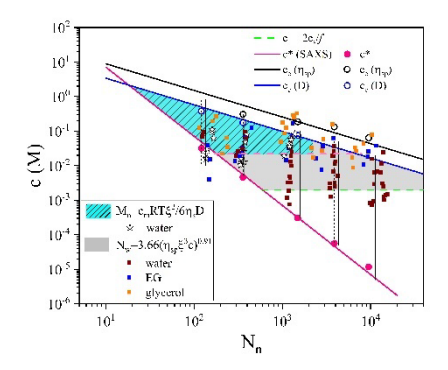
²Department of Chemistry and Macromolecules Innovation Institute, Virginia Tech,

Blacksburg, VA 24061

³Department of Chemistry, The Pennsylvania State University,

University Park, PA 16802

For Table of Contents use Only



Abstract

Chain dynamics in the semidilute unentangled regime can be used to determine the molecular weight of polyelectrolytes based on the Rouse scaling model. Four methods enable determination of the number density of chains via measurements of correlation length (ξ) by SAXS, specific viscosity (η_{sp}) and relaxation time (τ) by rheometry, and diffusion coefficient (D) by NMR. Five narrow dispersity cesium polystyrene sulfonate (CsPSS) solutions without salt are studied in water,

anhydrous ethylene glycol and anhydrous glycerol to test all methods. Combining viscosity and

correlation length yields the weight-average molecular weight (M_w) from the Rouse model.

Combining diffusion coefficient and correlation length in water provides number-average

molecular weight (M_n) reliably for chains with N < 2000 repeat units. Glycerol slows relaxation

dynamics, and the shear rate dependence of viscosity yields reliable τ for CsPSS with N >100,

which is governed by the product of z-average and z+1 average molecular weight (M_zM_{z+1}) in the

Rouse model. Terminal modulus $G = (\eta - \eta_s)/\tau$ via rheometry correlates with M_w/M_zM_{z+1} .

Keywords: Rheology, NMR diffusometry, Viscosity, Terminal Modulus, Relaxation Time

1. Introduction

Polyelectrolyte solutions were classified as the "least understood form of condensed matter" by

Nobel Laureate de Gennes. It has been known for a long time that polyelectrolyte chains in solution

without salt present have a very large conformational size due to the electrostatic repulsion

between ionizable groups along the chain.^{1, 2} Consequently, polyelectrolyte solution properties

differ greatly from neutral polymer solutions.³ The conventional molecular weight characterization

methods developed for neutral polymers including osmometry, light scattering and size exclusion

chromatography (SEC) are challenging to directly apply to polyelectrolytes. First, these techniques

usually measure the molecular weight in dilute solution. The overlap concentration ($c^* \sim N^{-2}$) is

very low for polyelectrolyte solutions without salt, making dilute measurements impractical for

long chains. Addition of salt is required for SEC to reduce the coil size and screen the electrostatic

interactions between macroions and the stationary phase that also contains ionizable groups.

2

However, aqueous SEC typically exhibits a huge error, since its universal calibration curve is usually established using neutral water-soluble polymers such as poly(ethylene oxide) or dextrans.⁴ Sodium polystyrene sulfonate (NaPSS) standards can also be used for universal calibration at various ionic strength, but assuming these universal calibration curves can be applied to different polyanions and polycations might still be misleading. Mori pointed out that early elution of NaPSS is affected by ion exclusion, and the hydrophobic interaction dominates between polyelectrolytes and column substrate materials.⁵ The challenges for static light scattering come from the multicomponent nature of polyelectrolyte solutions. The refractive index increment (dn/dc) value for polyelectrolyte solutions at constant salt concentration differs from that at constant chemical potential.⁶⁻⁸ Vrij and Overbeek⁶ found the refractive index increment at a constant salt concentration (dn/dc)_{cs} is different from that at a constant chemical potential (dn/dc)_{µs} for poly(methacrylic acid) and using (dn/dc)_{cs} causes huge error in M_w extrapolation using a Zimm plot. In order to obtain (dn/dc)_{µs}, the polyelectrolyte solutions have to be dialyzed against salt solutions so that the salt ions redistribute across the membrane.⁸

Osmometry is used to measure number-average molecular weight (M_n) of neutral polymers in dilute solutions. The osmotic pressure (Π) for polyelectrolyte solutions, however, includes contributions from both polyions and dissociated counterions. The osmotic pressure is proportional to the concentration of all solute species due to the gain of mixing entropy. Thus, dissociated counterions dominate in polyelectrolyte solutions without salt and give a much larger Π than neutral polymer solutions at the same polymer concentration. Other methods such as NMR end-group analysis and matrix-assisted laser desorption/ionization (MALDI) mass spectrometry are limited to low molecular weight polymers (< 25 kg/mol) and hence are not ideal methods. Thus, new techniques for determining the molecular weights of polyelectrolytes are necessary to

further advance their fundamental understanding as well as enable rapid development of new polyelectrolyte chemistries and their related technologies.¹⁷⁻²¹

In this work, we develop generic methods based on the Rouse scaling model to determine the molecular weight of polyelectrolytes in the semidilute unentangled regime because a wide concentration regime is expected for polyelectrolytes without salt.³ To test our methods, we purchased five different molecular weights of sodium polystyrene sulfonate (NaPSS) with narrow molecular weight distribution and ion-exchanged sodium to cesium counterions. This exchange provides better electron contrast for correlation length measurements using small-angle X-ray scattering. Water, anhydrous ethylene glycol (EG) and anhydrous glycerol are used as solvents²² to study various solution properties of cesium polystyrene sulfonate (CsPSS). Anhydrous EG and glycerol slow down relaxation dynamics, which enables us to study the dynamic properties using steady-state shear rheology, while water provides low viscosity and the least spectrally crowded solvent for diffusion measurements by NMR.

Background Theory for Semidilute Unentangled Polyelectrolyte Solutions

The scaling theory of polyelectrolyte solutions pioneered by de Gennes, *et al.* and further developed by Dobrynin, *et al.* predicts the dynamic properties of polyelectrolyte solutions over a wide concentration range.^{1, 2} The correlation length of the semidilute unentangled regime in the low salt limit is expected to follow the concentration dependence of $c^{-1/2}$ as shown in Eq. 1,

$$\xi = \left(\frac{B}{cb}\right)^{1/2} \left[1 + \frac{2c_s}{fc}\right]^{1/4} \tag{1}$$

where B is the chain contraction factor defined as the ratio of the fully extended length Nb and the actual chain contour length L, B = Nb/L, c is the number density of monomers of size b, c_s is the number density of each monovalent salt ion and f is the fraction of monomers with a dissociated counterion, making $2c_s/fc$ the ratio of salt ions and dissociated counterions. The low salt limit has $2c_s/fc << 1$ while the high salt limit has $2c_s/fc >> 1$. The chains in semidilute solution are random walks of N/g correlation blobs^{1,2} (N is the number of monomers in a chain and g is the number of monomers in a correlation blob, $g = c\xi^3$) with end-to-end distance R shown in Eq. 2.

$$R \cong \left(\frac{b}{Bc}\right)^{1/4} N^{1/2} \left[1 + \frac{2c_s}{fc}\right]^{-1/8}$$
 (2)

Since the electrostatic and hydrodynamic interactions are screened for length scales beyond ξ , the Rouse model is used to describe the relaxation dynamics (with characteristic relaxation time τ) of the chain of correlation blobs¹

$$\tau \cong \frac{\eta_s b^3}{kT} B^{-3/2} N^2 (cb^3)^{-1/2} \left[1 + \frac{2c_s}{fc} \right]^{-3/4}$$
 (3)

making low salt polyelectrolyte solutions rheologically unique since τ *increases* on dilution. The chain's self-diffusion coefficient can then be derived¹

$$D \approx \frac{R^2}{6\tau} \approx \frac{BkT}{6\eta_s bN} \left[1 + \frac{2c_s}{fc} \right]^{1/2}$$
 (4)

making D in the low salt limit independent of chain concentration. The properties shown above consider the presence of additional salt, which can be ignored at high enough polyelectrolyte concentration, if polyelectrolytes are exhaustively dialyzed against deionized water to remove the extra salt. By taking the ratio of D and ξ^2 , both B and the salt correction term effectively cancel out, leading to Eq. 5.

$$D \cong \frac{ckT\xi^2}{6\eta_s N} \tag{5}$$

Equation 5 determines the self-diffusion coefficient of polyelectrolyte chains in a perfectly monodisperse system. The scaling model suggests Rouse dynamics apply for semidilute unentangled solutions and each chain diffuses independently. Thus, for a polydisperse system, we can simply sum up the diffusion coefficients of each species present

$$D = \frac{\xi^2 kT}{6\eta_s} \sum_{i} \frac{c_i}{N_i} = \frac{\xi^2 kT}{6\eta_s} \frac{c}{N_n} = \frac{\xi^2 RT}{6\eta_s} \frac{c_m}{M_n}$$
 (6)

where c_m is the total mass concentration (g/ml) and M_n is the number-average molecular weight, which we then solve for

$$M_{n} = \frac{c_{m}\xi^{2}RT}{6\eta_{s}D} \tag{7}$$

We can multiply τ and ξ^3 , which again cancels out B and the $\frac{2c_s}{fc}$ terms as shown in Eq. 8.

$$\tau \xi^3 \simeq \frac{\eta_s N^2}{c^2 kT} \tag{8}$$

The specific viscosity based on the scaling model is shown in Eq. 9. Substituting ξ^3 in Eq. 9 gives another relation which is free of B, f and c_s . Both η_{sp} and ξ can be measured experimentally. The only unknown parameter is again c/N.

$$\eta_{\rm sp} \equiv \frac{\eta - \eta_{\rm s}}{\eta_{\rm s}} \cong B^{-3/2} N (cb^3)^{1/2} [1 + \frac{2c_{\rm s}}{fc}]^{-3/4} \cong \frac{N}{c\xi^3}$$
(9)

The Rouse model in dilute solution predicts $\eta_{sp} \cong \phi N$ where ϕ is the volume fraction of monodisperse chains of N monomers. In a polydisperse solution each chain contributes independently, $\eta_{sp} = \sum_i \phi_i N_i = \phi N_w$. Hence, η_{sp} is governed by the weight-average $N_w^{23,\,24}$ which leads to a method to determine N_w as Eq. 10.

$$N_{w} = \eta_{sp} \xi^{3} c \tag{10}$$

The Fuoss law scaling of Eq. 9 expects $\eta_{sp} = (\frac{c}{c^*})^{1/2}$ in the low salt limit for $c^* < c < c_e$, where c^* is the overlap concentration and c_e is the entanglement concentration. This Fuoss law has been observed to work reasonably well for a wide variety of polyelectrolytes²⁵ and a recent model even accounts for subtle departures.²⁶ Lastly, terminal modulus is the reciprocal of the steady-state compliance, which is known to have N_zN_{z+1}/N_w dependence.^{24, 27} Therefore, the N dependence of terminal modulus (G = ckT/N is kT per chain for monodisperse polymers)^{1, 3} can be expressed as

$$G = \frac{ckTN_w}{N_z N_{z+1}} \tag{11}$$

The relaxation time $\tau = (\eta - \eta_s)/G$ is thus controlled by the product $N_z N_{z+1}$ as

$$\tau \xi^3 \cong \frac{\eta_s N_z N_{z+1}}{c^2 kT} \tag{12}$$

The correlation length is usually measured using small-angle X-ray scattering (SAXS) or small-angle neutron scattering (SANS).²⁸⁻³⁰ Drifford and Dalbiez performed light scattering experiments on salt-free NaPSS solutions and obtained the correlation length at much lower concentrations.³¹

All of the scattering results^{1, 3, 22, 29, 31-36} suggest that the concentration dependence of ξ for polyelectrolyte solutions in the low salt limit follows the same power law dependence of $c^{-1/2}$, as expected by Eq. 1.

The relaxation times of polyelectrolyte solutions in the low salt limit are unique in the semidilute unentangled regime as τ decreases with increasing concentration with a power law of $c^{-1/2}$. The shear rate dependence of viscosity of salt-free polyelectrolyte solutions that show shear thinning can reliably be used to measure τ , and many experimental results of various monodisperse polyelectrolyte solutions in the low salt limit find $\tau \sim c^{-1/2}$ in agreement with Eq. $3.^{22, 37-39}$

The chain self-diffusion coefficient measurements of neutral polymer in dilute solutions can be simply obtained by dynamic light scattering (DLS). However, for semidilute solutions, DLS measures the cooperative diffusion coefficients on the length scale of correlation blobs. ⁴⁰ For dilute polyelectrolyte solutions, multiple components are present including polyions, dissociated counterions and solvents. Analyzing the diffusion results from DLS can be complicated as two relaxation modes are always present in polyelectrolyte solutions without salt. ⁴¹⁻⁴³

Oostwal, *et al.* successfully performed pulsed-field-gradient nuclear magnetic resonance (PFG-NMR) diffusometry on sodium polystyrene sulfonate aqueous solutions and obtained reliable diffusion coefficients of polyelectrolyte solutions in the semidilute unentangled regime.⁴⁴ Thus, in this study, NMR diffusometry is used to determine self-diffusion coefficients in water.

Cesium polystyrene sulfonate (CsPSS) of five different molecular weights with narrow molecular weight distribution are investigated to test our models. Cesium is used as the counterion because it has higher electron contrast with solvent than sodium counterions, and this enables us to study the correlation length from SAXS experiments at our in-house facility at Penn State.

2. Experimental

2.1 Materials Five molecular weights of narrow distribution NaPSS were purchased from Scientific Polymer Products (Webster, NY; cat no. 622, 624, 626, 627 and 923). The molecular weight information of NaPSS provided by the manufacturer are reported in Table 1. We checked the molecular weights of NaPSS using static light scattering after dialysis. NaPSS was ion-exchanged from Na⁺ counterions to Cs⁺ counterions by adding 20 times excess cesium chloride salt (CsCl) in solution leading to 5% Na⁺ and 95% Cs⁺ statistically. The samples were exhaustively dialyzed by flushing at least 20 L of deionized water (Milli-Q) using a 400 mL Amicon® stirred cell (Millipore) under 30 psi argon. MWCO 100 kDa, 30 kDa, 10 kDa, 3 kDa and 1 kDa ultrafiltration membranes (Ultracel) were used for samples that we refer to throughout as 2876K, 1158K, 457K, 101K and 35K CsPSS, respectively. The dialyzed solutions were then freeze dried to remove water. The powder obtained after freeze drying was stored in a vacuum oven at 40°C overnight to remove residual water. The percent of sulfonation was also verified by ¹H NMR. Further details on the degree of sulfonation are presented in the supporting information.

Table 1. Molecular weights of five CsPSS samples converted from information provided by the manufacturer using aqueous SEC

M _n (kg/mol)	Mw (kg/mol)	$M_{ m w}/M_{ m n}$	%Sulfonation ^a	%Sulfonation
				(NMR)
42.1	49.2	1.17	91	100
125	130	1.04	87	100
549	588	1.07	99	90
1099	1231	1.12	95	89
2807	3338	1.19	97 ^b	100

^a %Sulfonation is measured from elemental analysis and the values are given by the manufacturer. ^b% sulfonation is determined by titration by the manufacturer.

To test the polydispersity effects, we made two mixtures of 20/80 and 50/50 wt% 2876K/35K CsPSS in ethylene glycol solutions for rheology measurements. The weight-average degree of polymerization (N_w) is measured by static light scattering. The number-average degree of polymerization (N_n) is calculated based on the dispersity reported in **Table 1**. The z-average (N_z) and z+1-average (N_{z+1}) degrees of polymerization are estimated assuming a Shultz distribution for pure samples, 9 enabling all averages to be estimated for the mixtures.

- 2.2 Static Light Scattering A Brookhaven BI-200SM SLS/DLS instrument was used to check the weight-average molecular weights of NaPSS over angles ranging from 40 to 140 ° using a 641 nm diode laser. NaPSS was dialyzed to remove residual salt prior to making aqueous solutions with 0.1 M NaCl and 0.5 M NaCl. The differential refractive index (dn/dc) was determined for each molecular weight using a Brookhaven differential refractometer with a 620 nm laser for 0.1 M NaCl (see Fig. S1 in Supplementary Information). The $(dn/dc)_{\mu_S}$ for 0.5 M is extrapolated from literature values to 641 nm wavelength. ^{45, 46} Zimm plots were generated for each molecular weight to determine M_w , second virial coefficients (A₂) and radius of gyration (R_g).
- **2.3 Small-Angle X-Ray Scattering** The small-angle X-ray scattering was performed using a Xenocs Xeuss 2.0 SAXS/WAXS system with Cu radiation ($\lambda = 1.54$ Å) at Penn State's Materials Characterization Lab. The solution samples are loaded in a stainless-steel liquid cell sealed by two Kapton films with 1.2 mm pathlength and 1 hour exposure time. A Pilatus Hybrid CMOS two-dimensional SAXS detector was used to collect the scattered X-ray signals with a sample-to-detector distance of 2520 mm covering a q range from 0.1 to 1 nm⁻¹.
- **2.4 Rheology** The shear rate dependence of viscosity was measured using a strain-controlled Rheometrics Fluids Spectrometer (RFS-III) with a concentric cylinder geometry. The temperature

for all measurements was maintained at 25.0 °C using an external Julabo circulating water bath. For solutions with Newtonian viscosity $\eta_0 > 0.01$ Pa s, a concentric cylinder geometry with 13 mm bob length, 16.5 mm bob diameter and 17 mm cup diameter was used. For solutions that have lower viscosities, a larger concentric cylinder with 34 mm bob length, 32 mm bob diameter and 33 mm cup diameter was used to keep the measured torque above the minimum torque of the 100FRT force rebalanced transducer (0.002 g cm).

For low concentrations in water, as the solution viscosity approaches the viscosity of water and no shear thinning can be observed in the measurable shear rate range of the rheometer, a Cannon-Ubbelohde viscometer (CUC-75) was used to measure a more precise viscosity. The glass viscometer was immersed in a Boekel Grant water bath and temperature was maintained at 25.00 °C. This viscometer was also used to obtain the intrinsic viscosity of each molecular weight of NaPSS in aqueous 0.1 M and 0.5 M NaCl. We made sure $\dot{\gamma}\tau$ is smaller than 0.3 but $\dot{\gamma}\tau$ for the 2297K NaPSS in 0.1 M NaCl ranges from 0.2 to 0.5. Thus, the intrinsic viscosity of 2297K NaPSS in 0.1 M NaCl was determined using the larger RFS-III concentric cylinder instead.

2.5 Pulsed-Field-Gradient NMR Diffusometry

¹H PFG-NMR diffusometry was performed to determine the self-diffusion coefficients of the polyelectrolytes in salt-free water solutions. A 400 MHz Bruker Avance III WB NMR spectrometer, equipped with a MIC probe coupled to a Diff50 single-axis (z) gradient was mainly used for CsPSS molecular weights below 1100K. For concentrations below 0.01 M of all molecular weights, an 850 MHz Bruker Avance III HD NMR spectrometer, equipped with a MIC probe coupled to a Diff30 single-axis (z) gradient was used for better signal sensitivity and shorter experiment time. The pulsed-gradient stimulated echo (PGSTE) pulse sequence⁴⁷ was used with a 90° RF pulse length of 4.5 μs for 400 MHz NMR measurements and 13.5 μs for 850 MHz

measurements. To confirm both spectrometers give the same D, solution concentrations in the range of 0.01 M to 0.02 M for each molecular weight were studied using both spectrometers.

The spin-lattice relaxation time (T_1) and spin-spin relaxation time (T_2) for polyelectrolyte chains were measured using the inversion-recovery and Carr-Purcell-Meiboom-Gill (CPMG) pulse sequences, respectively. The polyelectrolyte solutions have broad peaks (short T_2 relaxation times). A half sinusoid gradient pulse length δ from 0.785 ms to 3.14 ms (effective rectangular pulse length varied from 1 ms to 2 ms) and the post gradient delay > 1 ms in the pulse sequence were used for 1 H diffusion measurements. The diffusion time Δ was varied from 25 ms to 200 ms depending on the molecular weight. The minimum gradient strength applied was in a range of 70-200 G/cm to significantly diffusion weight (reduce) the water peak intensity on the first slice of the PGSTE experiment. The maximum gradient strengths were adjusted from 200-2000 G/cm to achieve at least 90% of signal attenuation in 16-32 steps. The acquisition times were adjusted to be greater than a factor of three times the signal dephasing in the FID (T_2), and the relaxation delay time was optimized to 2 s to get maximum signal-to-noise ratio for the polymer peaks with minimum experimentation time. 8-15 Hz line broadening was applied during data processing to reduce excessive acquisition noise. All NMR measurements were performed at $25 \pm 1^{\circ}$ C.

3. Results and Discussion

Static Light Scattering

The molecular weights of as-received NaPSS samples were checked by static light scattering (SLS) in 0.1 M and 0.5 M NaCl/water to confirm the molecular weights reported by the manufacturer. **Fig. 1** shows an example Zimm plot made for 2297K NaPSS in 0.1 M NaCl. The dn/dc value is determined as the slope of the difference in refractive index (Δ n) plotted as a function of concentration in Fig. S1, which is found to be 0.187 \pm 0.0012 ml/g for 2297K NaPSS and 0.2026

 \pm 0.0008 ml/g for the other four lower molecular weight NaPSS. The Zimm plots for the other four NaPSS samples in 0.1 M NaCl are also reported in supplementary information (Fig. S2). The Mw values of original NaPSS obtained from both SEC determined by the manufacturer and the Zimm plots are summarized in Table S1. The second virial coefficients (A2) and the radius of gyration (Rg) for NaPSS in 0.1 M NaCl of five molecular weights are reported in Table 2 below. We find the radius of gyration in nm Rg = 0.0656 $M_w^{0.50}$ for NaPSS in 0.1 M NaCl, shown in Fig. S3. Comparing the M_w from the manufacturer and M_w obtained from SLS, the difference between the two M_w values is lower than 5% for the two highest molecular weights. However, the difference is around 25% for the other three lower molecular weights. Table 2 uses the M_w from SLS and calculates M_n using dispersity from Table 1 as our reference M_n molecular weight values, which are also used as sample names. The molecular weights are also confirmed by performing SLS in 0.5 M NaCl and the results are reported in Table S1. We also consider Mark-Houwink relations for intrinsic viscosity from the literature in Fig. S4 and Table S4 which show good agreement with the molecular weight measured by SLS.

Table 2. SLS results of five NaPSS in 0.1 M NaCl						
M _w (kg/mol) NaPSS	M _w (kg/mol) ^a CsPSS	Error ^b	$A_2 \times 10^4$ (mol cm ³ /g ²)	R_{g} (nm)	M _n CsPSS ^c	
27	39.7	+26%	21.7	9.67	35K	
72	111	+24%	16.6	19.1	101K	
329	490	+20%	8.88	35.8	457K	
874	1310	-5.1%	7.13	52.6	1158K	
2297	3301	-2.4%	6.32	108	2876K	

^aM_w of CsPSS assumes the degree of sulfonation reported by the manufacturer and 95% Cs⁺ to Na⁺ conversion.

 $^{^{}c}M_{n}$ calculated from the CsPSS M_{w} by dividing by the SEC dispersity, listed in Table 1, and used as sample names throughout this article.

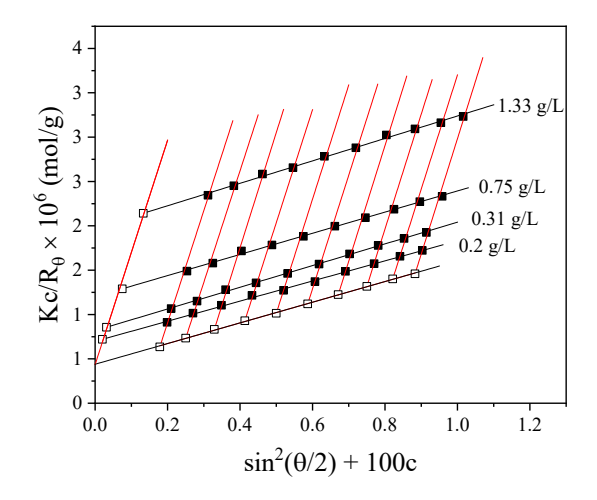


Figure 1. Zimm plot for 2297K NaPSS in 0.1 M NaCl. Filled symbols are data at the four indicated dilute concentrations and ten angles $\theta = 50$, 60, 70, 80, 90, 100, 110, 120, 130 and 140°. Open symbols are extrapolations to zero angle (at left) and zero concentration (at bottom).

Method 1: $N_w = \eta_{sp} \xi^3 c$

Method 1 measures the weight-average degree of polymerization N_w using Eq. 10, combining η_{sp} and ξ , which each can be easily measured using rheology and SAXS. The peak position q_{max} of SAXS profiles (shown in Fig. S5) determines the correlation length $\xi = 2\pi/q_{max}$ at different concentrations. ξ is plotted in **Fig. 2A** as a function of concentration and is clearly independent of

^bErrors are calculated for M_w obtained from SLS compared with the manufacturer reported M_w from aqueous SEC.

molecular weight in the semidilute unentangled regime. 1,2,9 For 35K CsPSS aqueous solutions, a dilute-semidilute crossover occurs at $c^* \sim 0.04$ M where $\xi \sim c^{-1/3}$ crosses to $\xi \sim c^{-1/2}$. Thus, for 35K CsPSS with $c < c^*$, the peak q_{max} in SAXS represents the average distance between chains in dilute solution. Although c^* can be easily determined for 35K aqueous solutions (0.04 M), it is harder for the other four higher molecular weights to determine c^* directly using the SAXS data because the peak cannot be resolved at lower concentration. The scattering peaks move to lower q as concentration decreases, and the low-q upturn in the SAXS profile eventually covers the entire weak peak as shown in Fig. S5. We applied the method by Kaji *et al.* to estimate c^* for other molecular weights as shown in Fig. 2B. 33 In the dilute regime, the distance between chains can be expressed as $(c/N)^{-1/3}$, where c/N is the number density of chains.

Therefore, ξ is plotted as a function of c/N_n in **Fig. 2B** and all datasets should cross to the same $(c/N_n)^{-1/3}$ dependence as the solution enters the dilute regime, which is set by the dilute results from 35K. The intercept of extrapolated $(c/N_n)^{-1/2}$ and $(c/N_n)^{-1/3}$ gives an estimate of c^* for each molecular weight in water with no salt present.

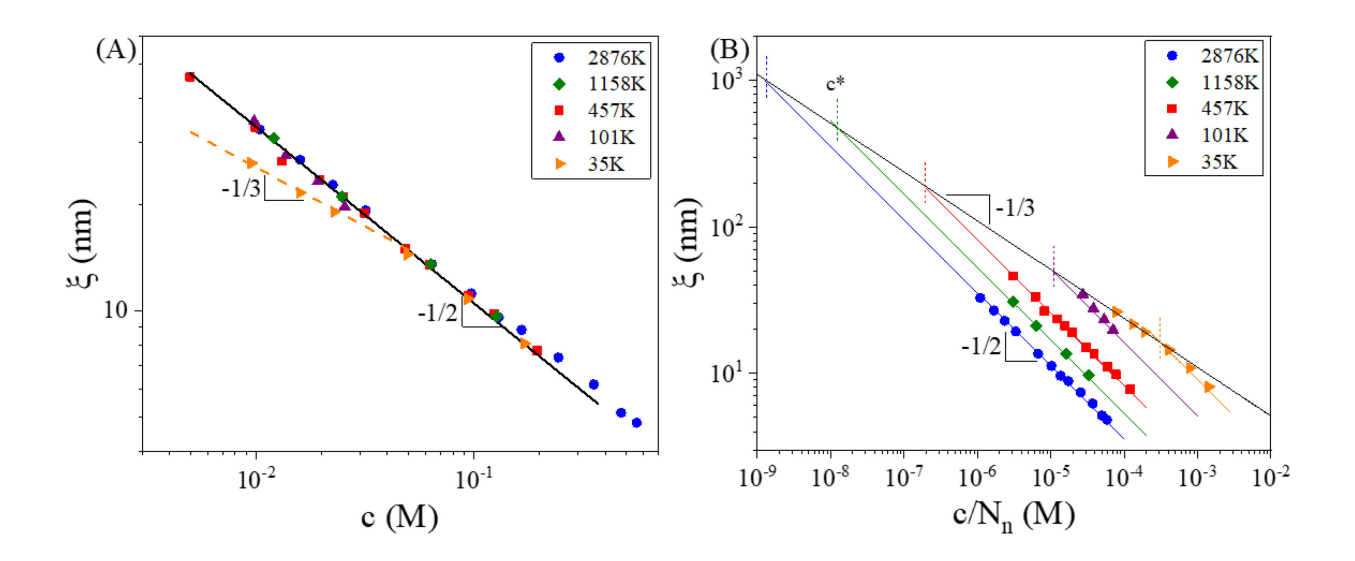


Figure 2. (A) Correlation length of CsPSS aqueous solutions as a function of concentration (moles of repeat units per liter) for five different molecular weights. 35K CsPSS reached the dilute regime for $c < c^* = 0.04$ M where the correlation length becomes the average distance between chains and can be fitted to a power law of $\xi \sim c^{-1/3}$. (B) Correlation length of CsPSS aqueous solutions as a function of chain number density (number density of monomers c normalized by number-average degree of polymerization N_n). The crossover from $c^{-1/3}$ to $c^{-1/2}$ estimates the overlap concentration c^* for each molecular weight with no salt present.

The data in **Fig. 2A** fit the line shown, as $\xi = A/\sqrt{c}$, with A = 3.37 nm·M^{1/2} for CsPSS in water. Similar fittings from the literature yield A = 3.30 nm·M^{1/2} for NaPSS in water,^{32, 48} A = 3.90 nm·M^{1/2} for CsPSS in EG and A = 3.80 nm·M^{1/2} for CsPSS in glycerol.²²

Fig. 3A shows specific viscosity η_{sp} as a function of polyelectrolyte concentration for CsPSS of five different molecular weights, to determine the semidilute unentangled regime where η_{sp} scales as $c^{1/2}$. For 101K and 35K CsPSS aqueous solutions, the semidilute unentangled scaling of $\eta_{sp} \sim c^{1/2}$ extends to concentrations far below c^* determined by SAXS, suggesting that Rouse dynamics still might apply in a range of concentrations in dilute solution. c^* and c_e as a function of number-average degree of polymerization are shown in Fig. 3B. The c_e is obtained from the crossover concentration from $\eta_{sp} \sim c^{1/2}$ to $\eta_{sp} \sim c^{3/2}$ because Method 1 fails for entangled solutions with $\eta_{sp} \sim c^{3/2}$ (see Fig. 3A).

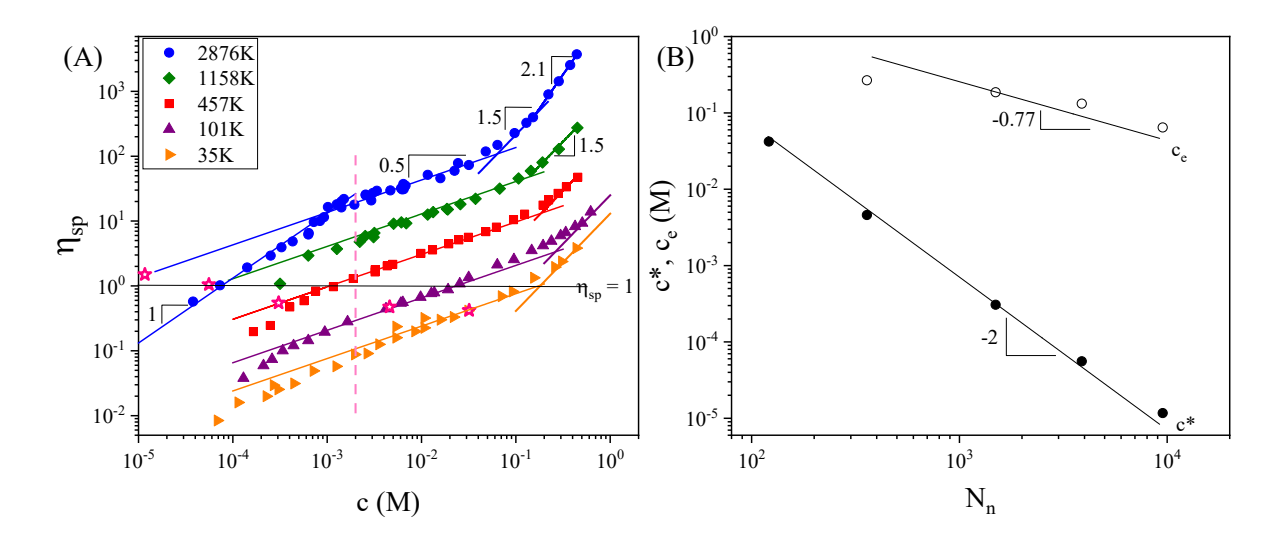


Figure 3. (A) Specific viscosity of CsPSS aqueous solutions with no added salt as a function of concentration for five different molecular weights. The solid lines are fits to power laws of c^1 for the dilute regime, $c^{1/2}$ for the semidilute unentangled regime and $c^{1.5}$ for the crossover to entangled solutions. Pink stars denote the c^* obtained from **Fig. 2B**. The pink vertical dashed line is an estimate of the border between the high and low salt limits at $2c_s/f = 0.002$ M, assuming f = 0.2 and f = 0.2 and f = 0.2 M (estimated later in Fig. 5). (B) Overlap concentration f = 0.2 oncentration (f = 0.2 as functions of number-average degree of polymerization (f = 0.2 solutions). f = 0.2 from f = 0.2 fro

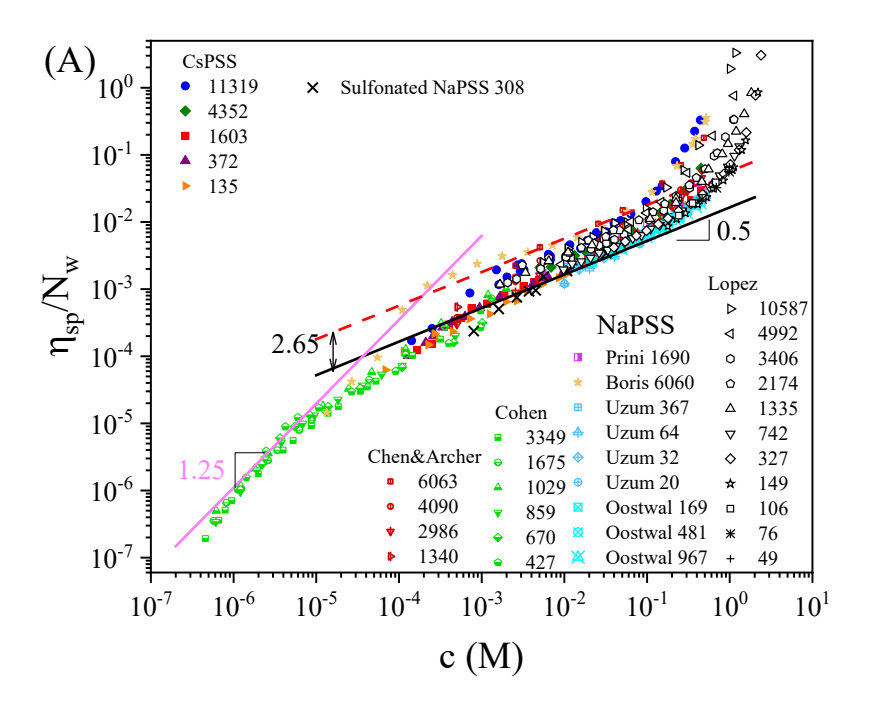
The scaling model predicts $\eta_{sp} \sim N_w$ (weight-average degree of polymerization) based on Rouse dynamics in the semidilute unentangled regime.^{1, 9} To test the N dependence of η_{sp} for aqueous polyelectrolyte solutions, η_{sp} is first normalized by N_w and plotted as a function of concentration as shown in **Fig. 4A**, which includes CsPSS from this study and NaPSS from the literature that studied NaPSS with no added salt.^{37, 49-55} It is worth noting that all polystyrene sulfonate samples plotted in **Fig. 4A** are from sulfonation of polystyrene with less than 100% degree of sulfonation.

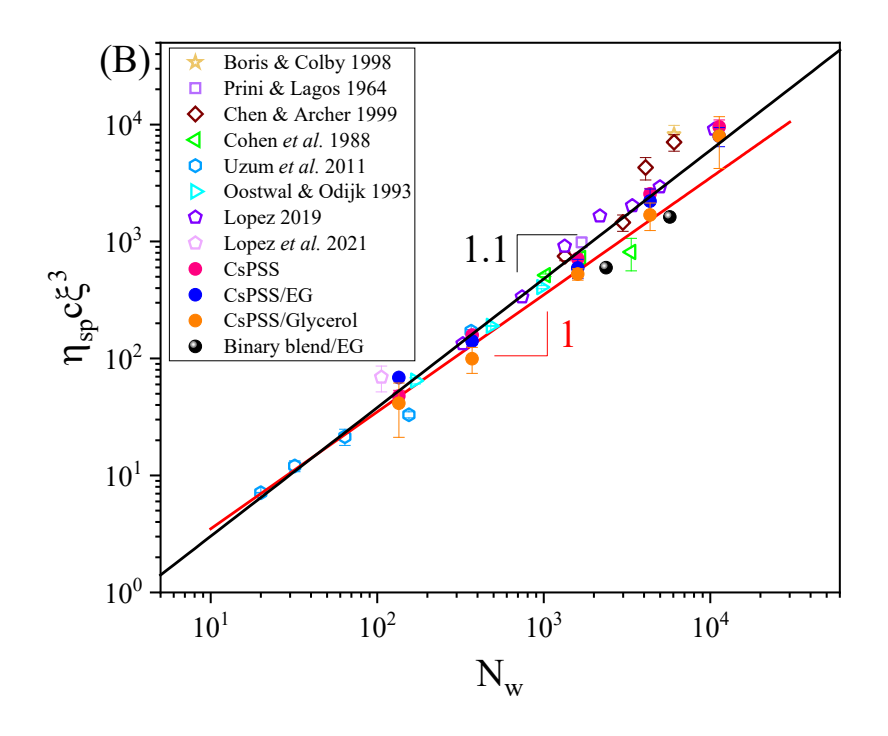
The molecular weight of the repeat unit from each source is calculated according to its respective degree of sulfonation. We also include one NaPSS ($N_w = 308$) that we sulfonated from a known molecular weight polystyrene, synthesized by anionic polymerization. The N_w value used is directly that of polystyrene so that degree of sulfonation does not affect the N_w calculation. For $N_w < 2000$, the data can be nicely reduced to a common curve where $\eta_{sp} \sim c^{1/2}$ for $c > 5 \times 10^{-4}$ M, as expected in the semidilute unentangled regime. For $N_w > 2000$, η_{sp}/N_w no longer reduces the data. The expected η_{sp}/N_w from the scaling theory is plotted as a function of c as dashed lines in Fig. 4A with b = 0.255 nm, length of one repeat unit, and B = 1.74 (black dashed line) for CsPSS in water and B = 1.67 (red dashed line) for NaPSS in water obtained from the SAXS results. $^{22, 56}$ The expected η_{sp}/N_w is 2.65 times higher than experimental data for $N_w < 2000$. It is also worth noting that the scaling prediction (dashed line) nicely goes through the experimental data for the highest molecular weights ($N_w = 11319$, 8586, 6063 and 6060) perhaps suggesting that the long chain limit assumption of the scaling theory is satisfied. The results are relatively scattered, and thus do not show a consistent dependence of η_{sp} on N_w .

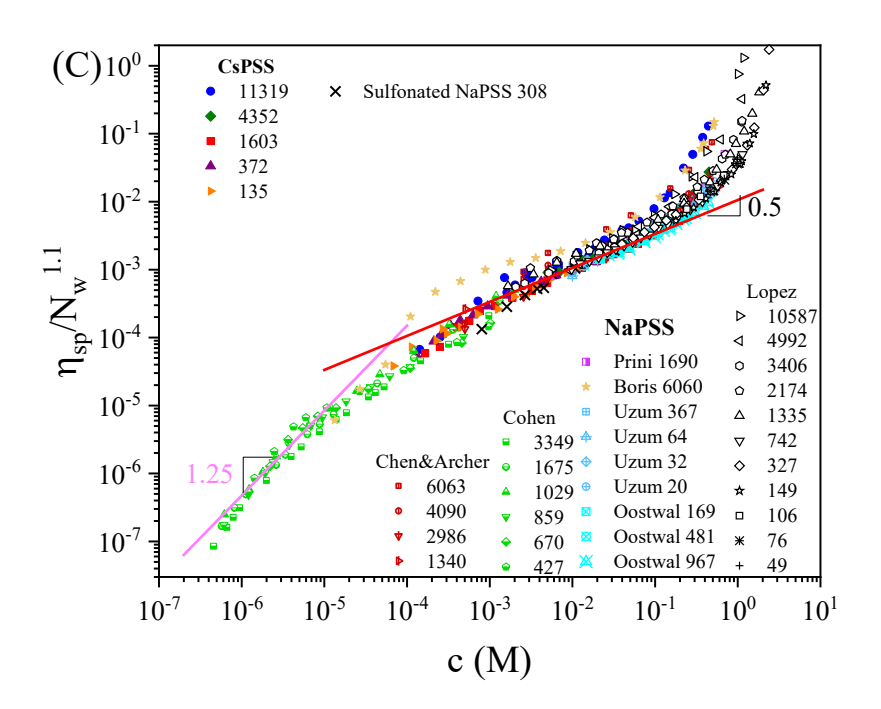
Hence, we plot $\eta_{sp}c\xi^3$ in the semidilute unentangled regime as a function of N_w as shown in **Fig.** 4B. $\eta_{sp}c\xi^3$ is dimensionless and **Fig.** 4B shows $\eta_{sp} \sim N_w^{1.1}$. The solid black line in **Fig.** 4B is the best fit to all data sets $(N_w = 3.66(\eta_{sp}c\xi^3)^{0.91})$ and it provides an easy measure of N_w for sulfonated polystyrene with any choice of counterions if one knows η_{sp} and ξ at a given semidilute unentangled concentration. The apparent scaling of $\eta_{sp} \sim N_w^{1.1}$ has been observed previously⁵⁵ and likely indicates a log correction to the Rouse scaling $(\eta_{sp} \sim N_w)$. In **Fig.** 4C $\eta_{sp}/N_w^{1.1}$ is plotted with far less scatter between data sets in water. We noticed the binary blend results are lower than pure component data for both 20 wt% 2876K/80 wt% 35K and 50 wt% 2876K/50 wt% 35K in **Fig.** 4B. Both blends show bimodal distribution. While the long chains are better fitted to $N_w^{1.1}$, the short

chains are generally fine with the N_w^1 dependence. Also, the non-uniform stretching shows stronger impact on longer chains than shorter chains.⁵⁷ Both blends contain more short chains (35K) than long chains (2876K), which makes the non-uniform stretching less pronounced comparing with a pure component solution that has the same N_w .

Figure 4D shows the concentration dependence of $\eta_{sp}/N_w^{1.1}$ in EG and glycerol is also reduced nicely for the five molecular weights. Like the aqueous data in Fig. 4C, the EG and glycerol data suggest a stronger concentration dependence than the Fuoss Law $c^{1/2}$. A best fit slope of 0.68 is shown as dashed red lines in Fig. 4D. Hence, our experimental result seems to be $\eta_{sp} \sim N_w^{1.1} c^{0.68}$ instead of the scaling prediction of $N_w c^{1/2}$.







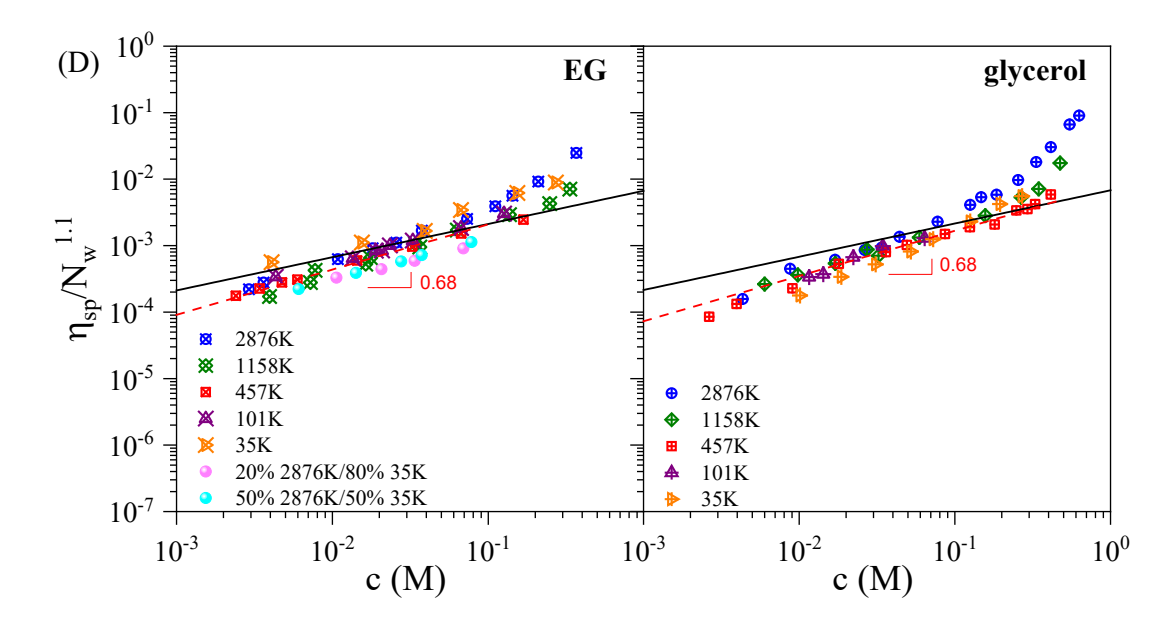


Figure 4. (A) Specific viscosity in water with no added salt, normalized by the weight-average degree of polymerization N_w for CsPSS from this work and for NaPSS from refs. 37 and 49-55. The legends show the N_w values used for normalization. We also sulfonated polystyrene, which is synthesized by anionic polymerization (black crosses). The blue dashed line is the expected η_{sp}/N_w based on Eq. 9 with b=0.255 nm and B=1.7 obtained from SAXS. The red dashed line is calculated with b=0.255 nm and B=1.67 for NaPSS without salt. For CsPSS, the expected η_{sp}/N_w is 2.65 times greater than η_{sp}/N_w obtained experimentally for $N_w < 2000$. The solid black line represents the best fit to the Fuoss law. (B) Direct test of Method 1: $\eta_{sp}c\xi^3$ as a function of N_w of CsPSS from this work and NaPSS from refs. 37 and 49-55 in the semidilute unentangled regime where $\eta_{sp} \sim c^{1/2}$ is observed. The Rouse model predicts specific viscosity to be a function of N_w alone for linear chains, and this correlation $\eta_{sp}c\xi^3=0.24N_w^{-1.1}$ is perhaps useful for estimating $N_w=3.66(\eta_{sp}c\xi^3)^{0.91}$. (C) Concentration dependence of $\eta_{sp}/N_w^{1.1}$ shows far superior data collapse for different molecular weights in water. The red solid line is $\eta_{sp}/N_w^{-1.1}=0.0106c^{1/2}$. The prefactor 0.0106 is calculated directly from the black solid line in part B. (D) $\eta_{sp}\sim N_w^{1.1}$ applied

to CsPSS in EG (left) and glycerol (right) data. The black solid lines are $\eta_{sp} / N_w^{-1.1} = 0.0067 c^{1/2}$ in EG and $\eta_{sp} / N_w^{-1.1} = 0.0068 c^{1/2}$ in glycerol, both calculated directly from the relation determined in part B, and show good agreement with data. It is worth noting that the best fit of the concentration dependence of η_{sp} is $\eta_{sp} \sim c^{0.68}$ (red dashed lines) for CsPSS/EG and CsPSS/glycerol, similar to the scaling exponent proposed by Chen *et al.*²⁵. The power law exponent of 0.68 also suggests another log correction due to non-uniform stretching should be considered for semidilute unentangled polyelectrolyte solutions.

We have also noticed in the concentration range of 10^{-5} M < c < 5 × 10^{-4} M of Fig. 4A, CsPSS data and NaPSS data measured by Cohen *et al.* show a slightly stronger concentration dependence of η_{sp} ($\eta_{sp} \sim c^{0.8}$). Cohen *et al.* found $\eta_{sp} \sim c^{1.25}$ for c < 10^{-5} M, which they say is caused by residual salt with $c_s \approx 4 \times 10^{-6}$ M.⁴⁹ To understand the intermediate concentration range, we plot the conductivity of solutions as a function of concentration in Fig. 5.

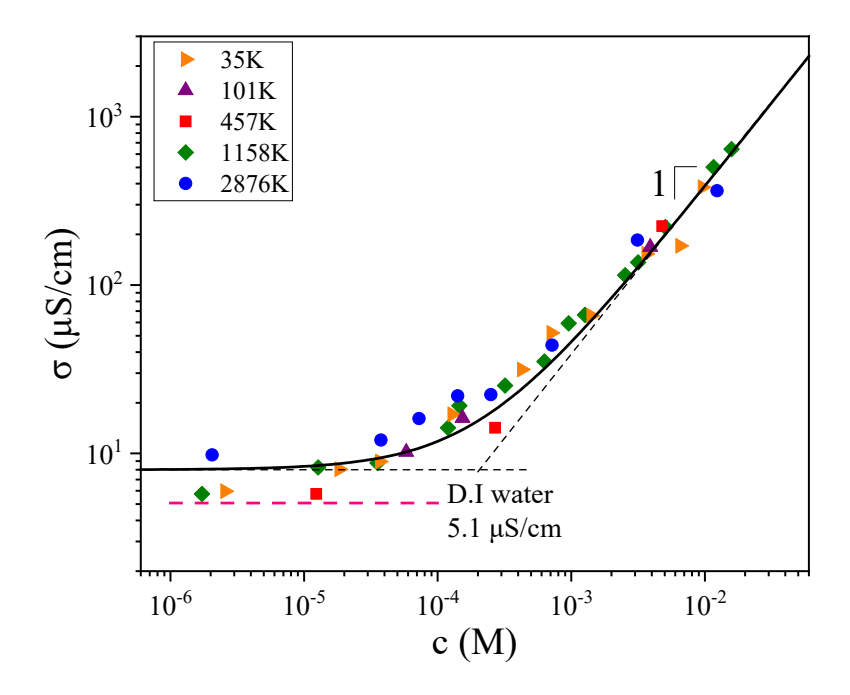


Figure 5. Ionic conductivity of CsPSS solutions at room temperature (22 °C). The pink dashed line indicates the conductivity of deionized water stored in a glass vial after 10 days. The crossover from $\sigma \sim c^0$ to $\sigma \sim c^1$ estimates the residual salt concentration c_s and the solid curve represents the fit to $\sigma = \sigma_0 (1 + c/c_s)$ where $\sigma_0 = 8 \,\mu\text{S/cm}$ and $c_s = 2.1 \times 10^{-4} \,\text{M}$.

The conductivity is measured after rheology measurements inside the concentric cylinder rheometry cup so that all residual salts can be examined by the conductivity measurements. The solution conductivity shows a concentration dependence of $\sigma \sim c$ for $c > 10^{-3}$ M and saturates around 8 μ S/cm at low concentrations. The conductivity data are fitted to the form of $\sigma = \sigma_0(1 + c/c_s)$, where σ_0 represents the conductivity of the high salt regime.⁵⁸ The possible sources of residual salts are ions from glass vials and carbonic acids, as CO_2 dissolves in water.⁴⁹ The transition from $\sigma \sim c$ to the plateau at 8 μ S/cm covers a decade of concentration, which might be

associated with the slightly stronger concentration dependence $\eta_{sp} \sim c^{0.8}$ in the range of 10^{-5} M < c $< 5 \times 10^{-4}$ M before entering the high salt regime at lower polymer concentrations.

Combining the information from Fig. 2A and Fig. 3A, the N_w values are calculated for each concentration using $N_w = 3.66 (\eta_{\rm sp} c \xi^3)^{0.91}$. The N_w from Method 1 is compared with the expected N_w value in Fig. 6.

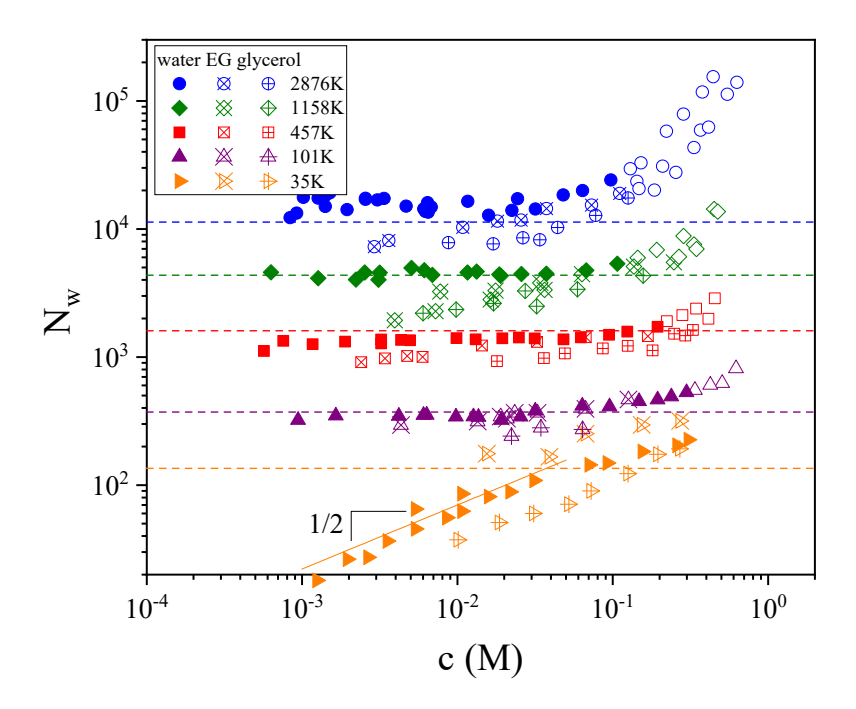


Figure 6. Weight-average degree of polymerization computed from Method 1 in three solvents. The dashed lines are the expected N_w reported in Table 2. The final N_w values (see Table S6) are determined by only using the concentrations where $\eta_{sp}\sim c^{1/2}$ but above c^* for each molecular weight. Open symbols denote entangled solutions where Method 1 cannot predict N_w .

In the semidilute unentangled regime for sulfonated polystyrene, the calculated N_w is independent of concentration, as expected. At higher concentrations, the increase of apparent N_w value is caused

by the entanglement effects (open symbols). For 35K CsPSS, this method exhibits N_w with a power law concentration dependence of $c^{1/2}$ below c^* (0.04 M). The calculated N_w values are only taken from the semidilute unentangled regime above c^* .

Method 2:
$$N_z N_{z+1} \cong \frac{\tau \xi^3 c^2 kT}{\eta_s}$$

The second method combines the relaxation times with correlation lengths based on Eq. 12. The relaxation time (τ) is obtained by fitting the shear rate dependence of viscosity curves to the Carreau model:

$$\eta(\dot{\gamma}) = \eta_0 [1 + (\tau \dot{\gamma})^2]^{(n-1)/2} \tag{13}$$

The aqueous solutions of 2876K and 1158K CsPSS show shear thinning, whereas the other molecular weights are Newtonian in the measurable shear rate range of the rheometer used. Therefore, ethylene glycol (EG) and glycerol were used as solvents to test this method on lower molecular weight samples because their viscosities are much higher, which effectively slow down the relaxation dynamics of polyelectrolyte chains in solution. The correlation lengths of CsPSS in EG and glycerol solutions were obtained from our previous work.²² The relaxation time of all molecular weights in the three different solvents are normalized based on Eq. 12, as shown in **Fig.** 7, and the normalized relaxation times of different molecular weights can be reasonably reduced to the expected power law dependence of c⁻². **Table 3** lists the N_n, N_w, N_z and N_{z+1} of all samples that are used for normalizing **Fig. 7**. The values of N_z and N_{z+1} are estimated from dispersity N_w/N_n assuming the Shultz distribution.

Table 3. Degrees of polymerization of pure CsPSS and mixtures				
	Nn	N_{w}	N_z	N_{z+1}
2876K	9517	11319	13129	14929
1158K	3885	4352	4817	5284

457K	1494	1603	1703	1808
101K	359	372	388	402
35K	121	135	150	165
20/80 2876K/35K	151	2372	12536	14921
50/50 2876K/35K	239	5729	12976	14927

Fig. 7 shows that the relaxation time obtained from the shear rate dependence of viscosity can be well reduced by N_zN_{z+1} , even for the binary mixtures. Therefore, the shear thinning behavior of a polydisperse unentangled solution is mainly governed by the high molecular weight tail of the distribution.

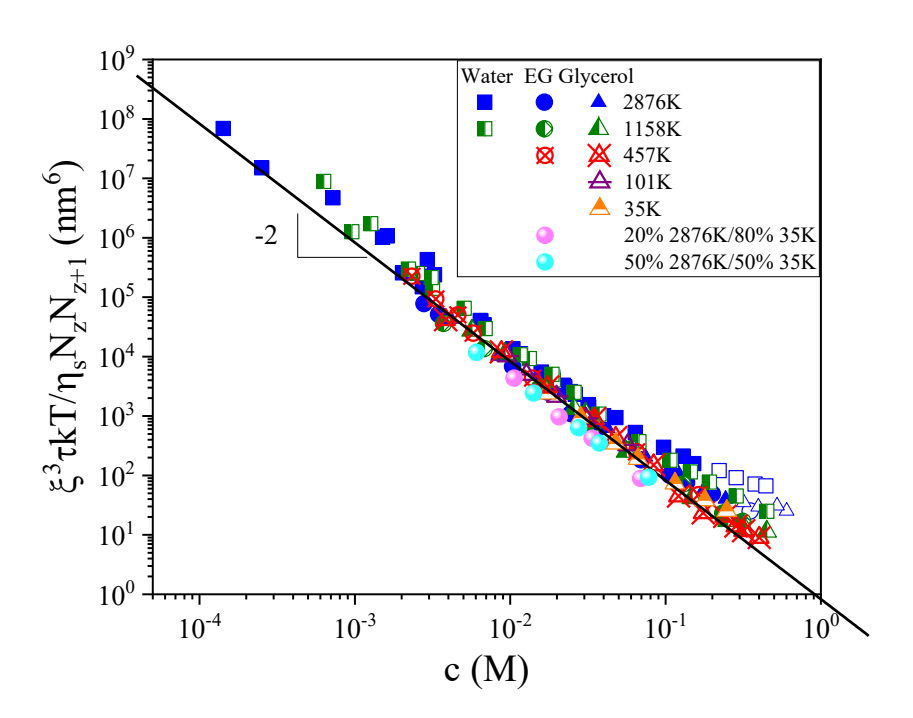


Figure 7. Relaxation times of CsPSS in three different solvents, obtained from fitting the shear rate dependence of viscosity to the Carreau model, normalized to a power law concentration dependence of $\xi^3 \tau k T/\eta_s N_z N_{z+1} \sim c^{-2}$. The solid black line represents the best fit to all data in the

semidilute unentangled regime with a power law dependence of c⁻². Entangled concentrations are plotted as open symbols and fall expectedly above the solid line.

Method 3:
$$\frac{N_z N_{z+1}}{N_w} = \frac{ckT}{G}$$

The third method utilizes the terminal modulus (kT per chain) to characterize the molecular weight of semidilute unentangled solutions. Fig. 8 shows $G = (\eta - \eta_s)/\tau$ as a function of cN_w/N_zN_{z+1} . All data are nicely collapsed onto the common line with a slope of unity. For narrowly distributed polyelectrolytes, it is hard to differentiate which moment of molecular weight distribution governs the terminal modulus. Thus, the two binary blend polydisperse systems are good examples to show that the terminal modulus, which is the reciprocal of steady state compliance, is controlled by N_w/N_zN_{z+1} as expected by the polydisperse Rouse model. This relation explains why ckT/ N_n overestimates G from previous works in polyelectrolyte solutions especially for slightly polydisperse systems S_y^{29} , where S_y^{29} is since the terminal modulus is mainly controlled by the high molecular weight tail of the molar mass distribution.

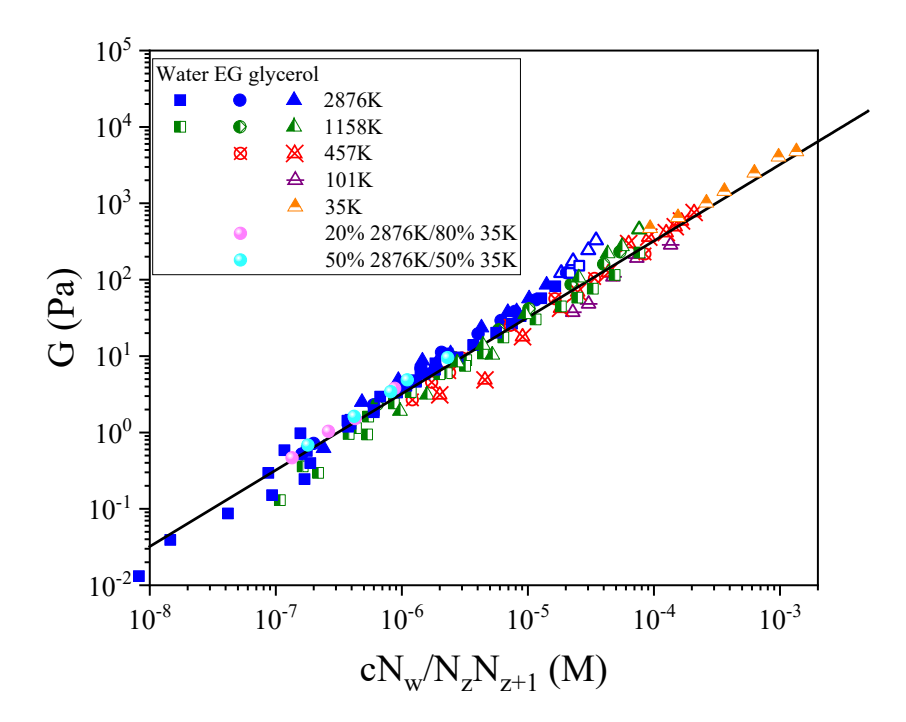


Figure 8. Terminal modulus of CsPSS for five molecular weights in water, EG, and glycerol. The solid line is the best fit to a slope of 1. Open symbols represent measurements above the entanglement concentration and fall expectedly above the line.

Method 4:
$$M_n = \frac{c_m RT \xi^2}{6\eta_s D}$$

The last method utilizes D and ξ to quantify the number density of chains. ¹H NMR spectra of CsPSS in water are first measured as shown in **Fig. 9**. The proton peaks of the polyelectrolyte (color coded, **Fig. 9A**) are well resolved from the large H₂O peak. The three major peaks are used for NMR diffusometry measurements to determine the self-diffusion coefficient of polyelectrolyte chains in solution. These three peaks are actually the overlap of many individual resonances due to the slow timescale of rotational polymer chain dynamics relative to small molecules in solution. Linewidths increase with molecular weight, as shown in **Fig. 9B**. More details of linewidth and its

consequences for NMR measurements of polyelectrolyte diffusion coefficient are discussed in the SI.

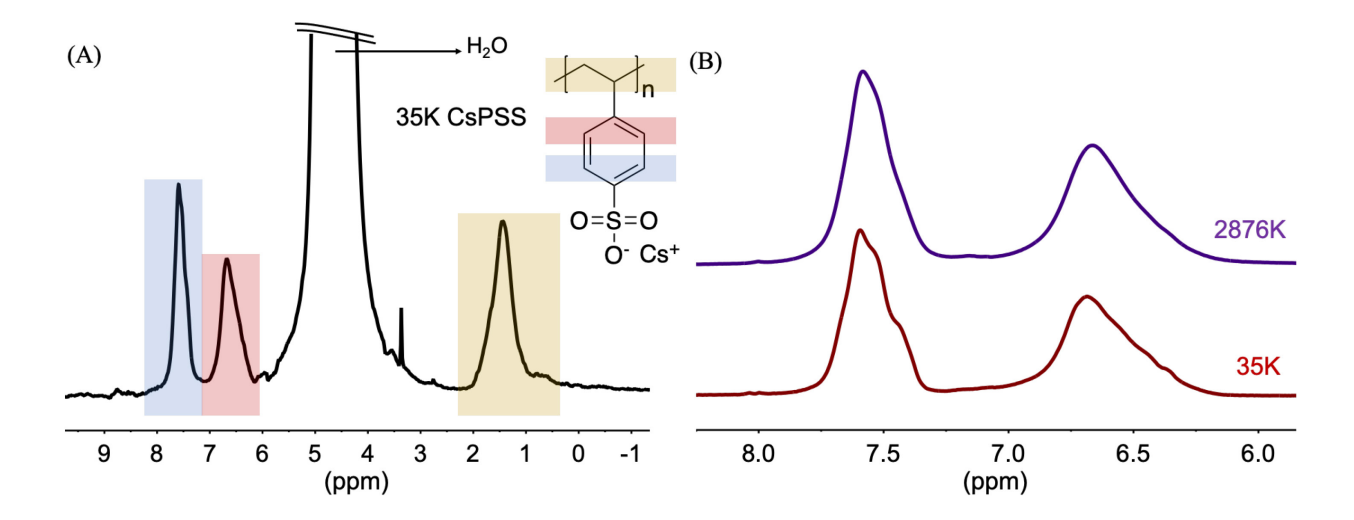


Figure 9. (A) 1 H NMR spectrum of 0.063 M of 35K CsPSS in H₂O measured at 25 ± 1°C (referenced at 4.8 ppm). The polymer proton peak assignments are shown using different colors. (B) is the zoomed-in 1 H NMR spectrum of 0.063 M 35K and 2876K CsPSS in D₂O (HOD peak referenced at 4.8 ppm) for better visualization of the two aromatic peak groups, which exhibit overlapping of many individual proton peaks. The linewidth increases with molecular weight, causing increased signal dephasing during the NMR diffusometry experiment and thus limiting measurement of D to concentrations above $\sim 4 \times 10^{-3}$ M for high M_n. For low M_n polymers, concentrations as low as $\sim 1 \times 10^{-3}$ M are accessible. See SI for further discussion of linewidth and D measurements.

The pulsed-gradient stimulated echo (PGSTE) pulse sequence was employed to evaluate the diffusion coefficient of chains for five different molecular weights, each as a function of concentration. The NMR signal intensity I for each peak was measured as a function of gradient

strength (g). The acquired signal dependence is given by the Stejskal-Tanner equation shown in Eq. 14 59

$$I = I_0 e^{-\gamma^2 g^2 \delta^2 \left(\Delta - \frac{\delta}{3}\right) D}$$
 (14)

where γ is the gyromagnetic ratio of the nucleus, δ is the effective gradient pulse length, Δ is the diffusion time between gradient pulses, I_0 is the signal intensity at g=0, and D is the self-diffusion coefficient of the species measured.

Fig. 10 shows representative NMR diffusometry signal attenuation (Stejskal-Tanner) plots for five molecular weights as a function of NMR diffusion parameter $b = \gamma^2 g^2 \delta^2 (\Delta - \delta/3)$. Five additional representative NMR signal attenuation plots for each molecular weight are shown in the SI, demonstrating that accurate D measurement is possible over these concentration ranges in water without salt. The $\ln(I/I_0)$ vs. b data can be fitted to a single linear regression, indicating that all samples have a single average diffusing species size with narrow distribution, and the slope corresponds to D.

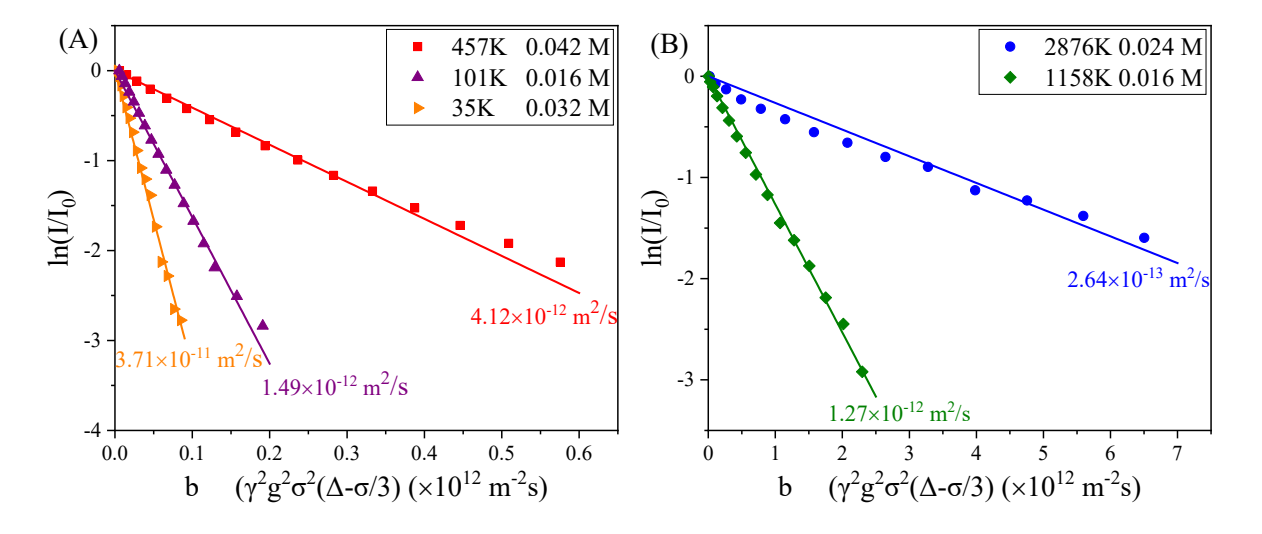


Figure 10. Representative NMR signal attenuation (Stejskal-Tanner) plots of CsPSS aqueous solutions of five different molecular weights in the semidilute unentangled concentration regime

obtained from the Bruker Avance III 850 MHz spectrometer. Solid lines are single exponential fits for each molecular weight at the indicated concentration.⁶⁰ The diffusion coefficient for each solution is shown next to the respective fit lines. Faster attenuation (steeper negative slope) of the lines correlate with faster diffusion (larger D). Additional signal attenuation plots spanning all concentrations and molecular weights are included in the SI (see Fig. S11).

The concentrations selected for **Fig. 10** are in the semidilute unentangled regime, and D is independent of concentration as shown in **Fig. 11(A)** for 35K, 101K and 457K. The decrease of D as the concentration increases indicates the entanglement effects that restrict the chain motion. The onset of the drop of *D* is marked by the black dotted line in **Fig. 11(A)**. For molecular weights 457K, 1158K and 2876K, we noticed a consistent increase of the diffusion coefficients as concentration decreases, which can be fitted to the power law exponent of -1/2 expected by Eq. 4, below a constant concentration (0.022 M). **Fig. 5** indicates the c_8 for our system is 2.1×10^{-4} M, associated with a Debye length (r_D) of 22 nm. **Fig 11(B)** compares r_D with ξ over the same range of concentration as **Fig 11(A)**. Solutions are apparently in the high salt regime at concentrations with $r_D < \xi$. The intersecting concentration between r_D and ξ is also at 0.022 M, confirming the high salt limit observed in **Fig. 11(A)**. Although the same high salt limit applies to 101K and 35K, the lower concentrations of these two lower molecular weight samples are dilute and D is concentration independent in the dilute regime with salt concentration constant.¹

For 1158K and 2876K CsPSS solutions, although plateaus are plotted as straight lines, a clear plateau was not observed for these two highest molecular weights. Thus, the range with D independent of concentration is too narrow and we cannot confidently define this region. Thus, Method 4 is better used at this time for N < 2000 for CsPSS. The diffusion coefficients of the

original NaPSS were also measured to test the effects of counterion on diffusion coefficient. NaPSS and CsPSS with the same chain length show the same diffusion coefficients in the semidilute unentangled regime, demonstrating that counterions do not affect the chain self-diffusion.

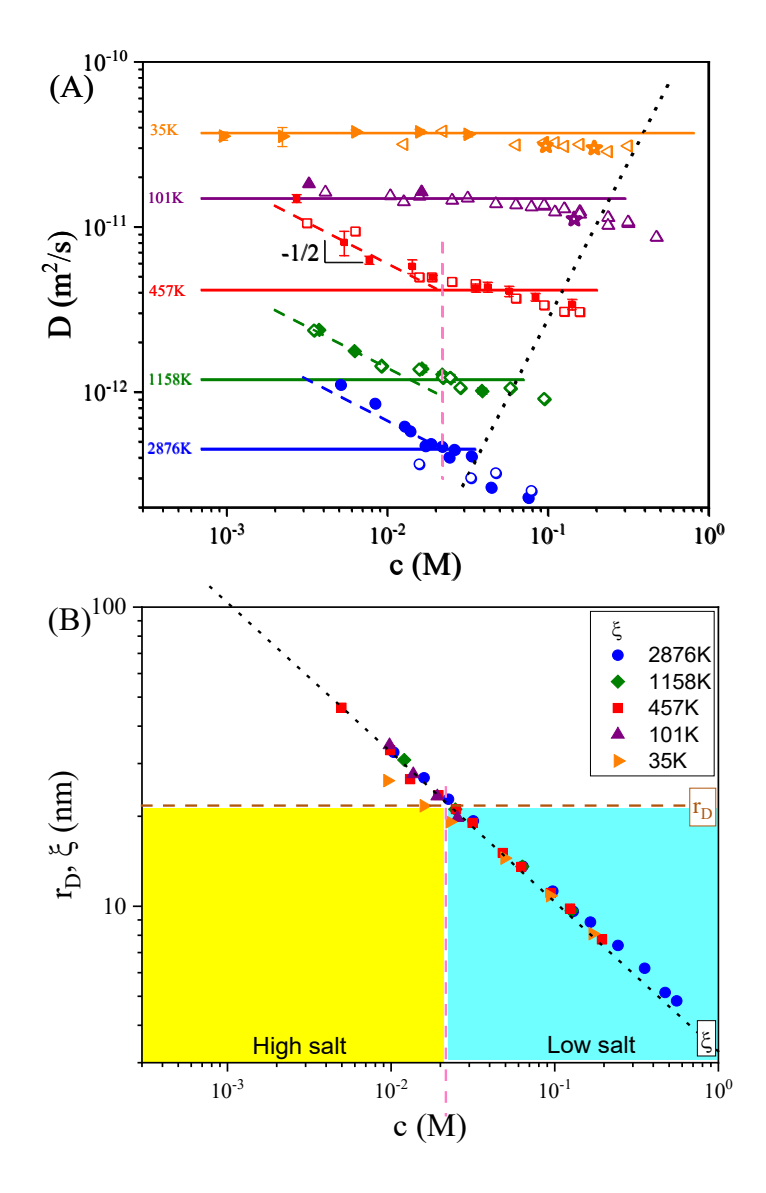


Figure 11. (A) Diffusion coefficients as a function of concentration for CsPSS/water solutions. The open symbols are obtained at 400 MHz, and the filled symbols are obtained at 850 MHz. The solid lines indicate the average D in the semidilute unentangled regime without salt effects. The

dotted black line indicates the entanglement concentration c_e . A few diffusion coefficients for NaPSS are also measured and plotted as stars. The dashed lines are fits to power law exponent of -1/2 which represents the high salt limit of Eq. 4. The vertical pink dashed line shows the crossover from $c^{-1/2}$ (high salt regime) to c^0 (low salt regime). (B)The Debye length r_D of 22 nm is determined with residual salt concentration $c_s = 2.1 \times 10^{-4}$ M from Fig. 5. The correlation length ξ equals $r_D = 22$ nm (brown dashed line) at c = 0.022 M (pink vertical dashed line in both parts). This same crossover is observed in (A): $D \sim c^{-1/2}$ crosses to $D \sim c^0$ at c = 0.022 M for 457K, 1158K and 2876K.

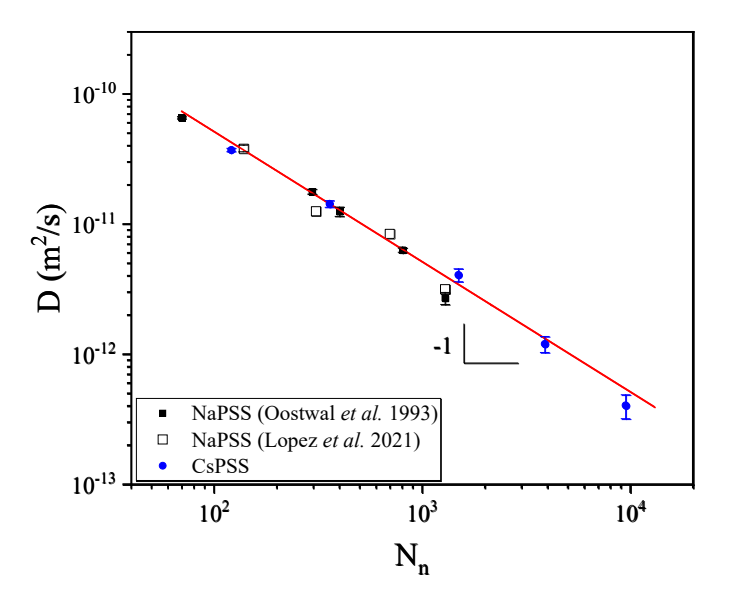


Figure 12. Diffusion coefficients in aqueous semidilute unentangled solutions as a function of number-average degree of polymerization of CsPSS in this work (blue circles), for NaPSS from ref. 44 (black filled squares) and from ref. 55 (black open squares). Error bars are calculated from the standard deviation of concentrations below c_e , as indicated by the black dashed line of **Fig. 11A**, and above the concentration c = 0.022 M, below which D starts to increase with decreasing concentration. The red line is the dependence of Eq. 6 ($D = kT\xi^2c/6\eta_sN_n$). The best fit of all data suggests a power law exponent of -1.03. A plot of $D(\eta - \eta_s)/c^{1/2}$ as a function of concentration (Fig S12) shows that although the N dependence of D and η_{sp} are both slightly stronger than the

expected exponent of 1, the product the two properties still follows Rouse dynamics and also agrees well with the expected concentration dependence of $R_{\rm g}$ from SANS.

The average diffusion coefficient in the semidilute unentangled regime where D is independent of concentration is plotted as a function of N_n in Fig. 12. The red line in Fig. 12 is $D = kT\xi^2c/6\eta_s N_n$ expected by Eq. 6. CsPSS data from this work agree well with NaPSS diffusion coefficient data from the literature, $^{44,\;55}$ and the data not only obey the Rouse scaling prediction 9 of $D\sim N_n^{-1}$ but even the numerical coefficient of Eq. 6 is correct! Eq. 5 suggests that DN_n should be concentrationindependent in the semidilute unentangled regime. In Fig. 13, the diffusion coefficients are multiplied by their respective N_n for CsPSS from this work and for NaPSS from ref. 44. We found that the normalized data can be reasonably reduced to a common line, and the concentrationindependent regime shows a constant value of $DN_n=4.66\times 10^{-9}\ m^2/s$ for CsPSS and $DN_n=4.86$ × 10⁻⁹ m²/s for NaPSS shown as green dashed lines. Oostwal, et al.'s work has shown that for high molecular weight NaPSS, the PFG-NMR data cannot be fitted to a single exponential due to the dispersity of molecular weights, and only the "initial decay" data were fitted with a single exponential function to obtain the diffusion coefficients in their study. 44, 61 The initial decay is associated with components that diffuse faster, dominated by the lower end of the molecular weight distribution and the slower diffusing components contribute more to the decay curve at higher b values. Therefore, the actual diffusion coefficients might be lower than Oostwal's reported values that are plotted in Fig. 13B for the high molecular weight samples.

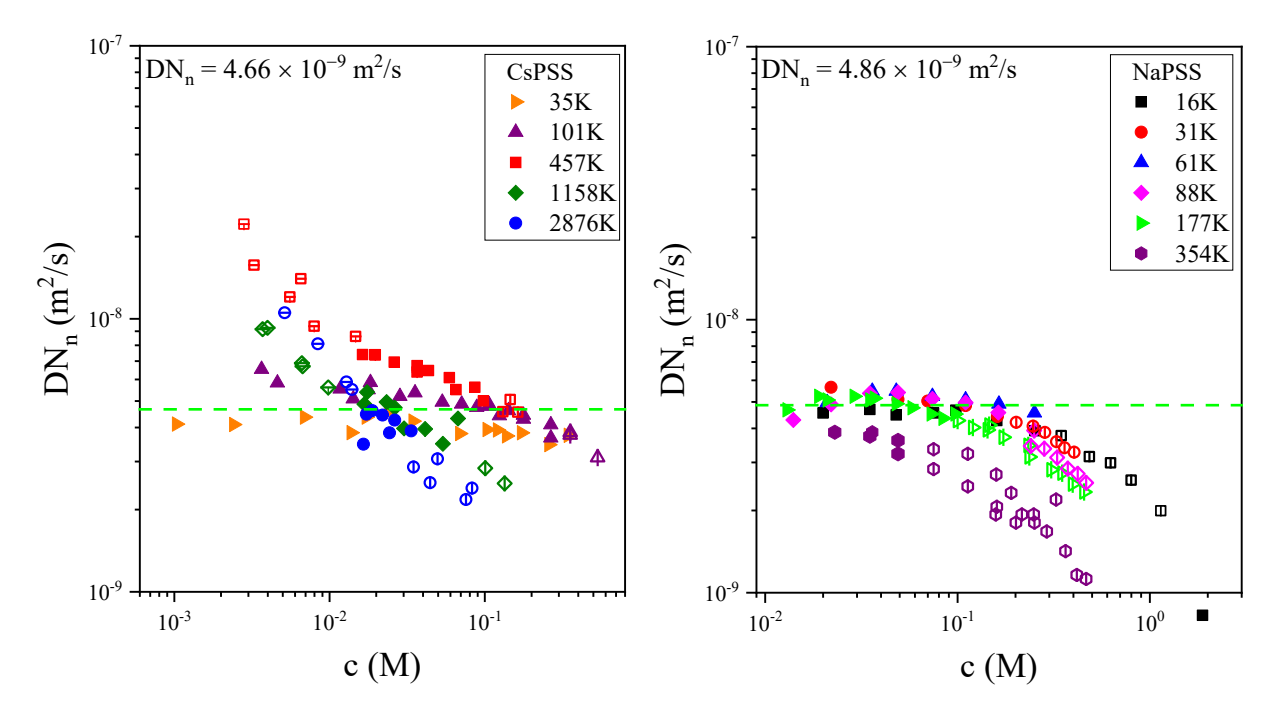


Figure 13. Diffusion coefficients in salt-free water normalized by number-average degree of polymerization N_n for CsPSS (A) from this work and NaPSS (B) from ref. 44. The legends indicate the M_n values for each molecular weight. The dashed lines are average DN_n for the semidilute unentangled regime. For 457K, 1158K, 2876K, concentrations below 0.022 M are plotted as open symbols with horizontal lines inside. Open symbols with vertical lines inside represent entangled solutions with $c > c_e$.

Conclusion

We have presented four methods to quantify the molecular weight of polyelectrolytes in semidilute unentangled solutions. Each method has its limitations regarding the range of molecular weights, as shown in **Fig. 14**. Method 1 ($N_w = 3.66(\eta_{sp}c\xi^3)^{0.91}$) gives the weight-average molecular weight based on the observed N_w dependence of η_{sp} as suggested by **Fig. 4B** $\eta_{sp}c\xi^3 \sim N_w^{1.1}$. The method is also tested for two binary blends at various concentrations which show good agreement.

Owing to the simplicity of measuring viscosity, Method 1 deserves more investigation in future work, to study the physical significance of the constant prefactor 3.66.

Methods 2 $(N_z N_{z+1} \cong \frac{\tau \xi^3 c^2 kT}{\eta_s})$ and 3 $(\frac{N_z N_{z+1}}{N_w} = \frac{ckT}{G})$ require measurements of chain relaxation time. We measure the relaxation time from the shear rate dependence of viscosity fit to the Carreau model and this method needs sufficient shear thinning to yield a reliable fit. This is more challenging for lower molecular weight samples and low viscosity solvents, due to the lack of shear thinning. This problem can be addressed by replacing water with higher viscosity polar solvents like EG and glycerol to measure the relaxation time for lower molecular weights. However, flow curves are not ideal for the lowest molecular weight CsPSS, as $10^4 \ s^{-1}$ shear rate would be required to obtain sufficient shear thinning data. The ideal way of determining relaxation times might be (1) performing oscillatory shear experiments and extrapolating the G' and G" slopes of 2 and 1 to where those power laws cross, or (2) measuring recoverable compliance J_e^o from creep recovery to calculate relaxation time as $\tau = \eta J_e^{\circ}$. These two methods are mainly governed by the high molecular weight tail of the distribution, which is important for highly polydisperse systems. Our data show great agreement with the polydisperse Rouse model, ^{24, 27} suggesting that the onset of shear thinning is controlled by N_zN_{z+1}, which physically means that shear thinning starts when the long chains get stretched by the shear flow.

Method 4 ($M_n = \frac{c_m RT\xi^2}{6\eta_s D}$) determines the number-average molecular weight and it shows promising results for relatively short polyelectrolytes with N < 2000. For 457K, 1158K and 2876K, the diffusion coefficient increases as concentration is lowered, which is most likely caused by residual salt. A clear plateau for 457K can still be observed for the semidilute unentangled regime for CsPSS solutions, as expected by the scaling model, before reaching the high salt limit. Since DN_n

is a constant in the semidilute unentangled regime for one type of polyelectrolyte, if one measures the D of a polyelectrolyte with unknown molecular weight, its N_n can be simply determined. Since NMR line widths increase with molecular weight and decrease with temperature, higher temperatures should be explored for diffusion measurements of polyelectrolytes with N > 2000. The high salt limit also needs to be avoided for high molecular weight samples, so that D is independent of concentration. At this time, it is not clear why the diffusion coefficient is so sensitive to residual salt, crossing between the high and low salt limits at c = 0.022 M, apparently where the correlation length reaches the Debye length from residual salt (pink dashed line in Fig. 11). The specific viscosity instead follows the expectation of Eq. 9, with the crossover between the high and low salt limits at $c = 2c_s/f = 0.002$ M. As we explore polydisperse polyelectrolyte solutions further, we will compare our predicted result that D yields M_n (Eq. 6) with previous observations that D measurement by NMR provides M_w for dilute polymer solutions.⁶¹⁻⁶³ Finally, we note that these four methods each probe different parameters of the molecular weight distribution for polyelectrolytes, thus enabling access to intricate and quantitative information about these materials that are challenging to study and yet technologically important.

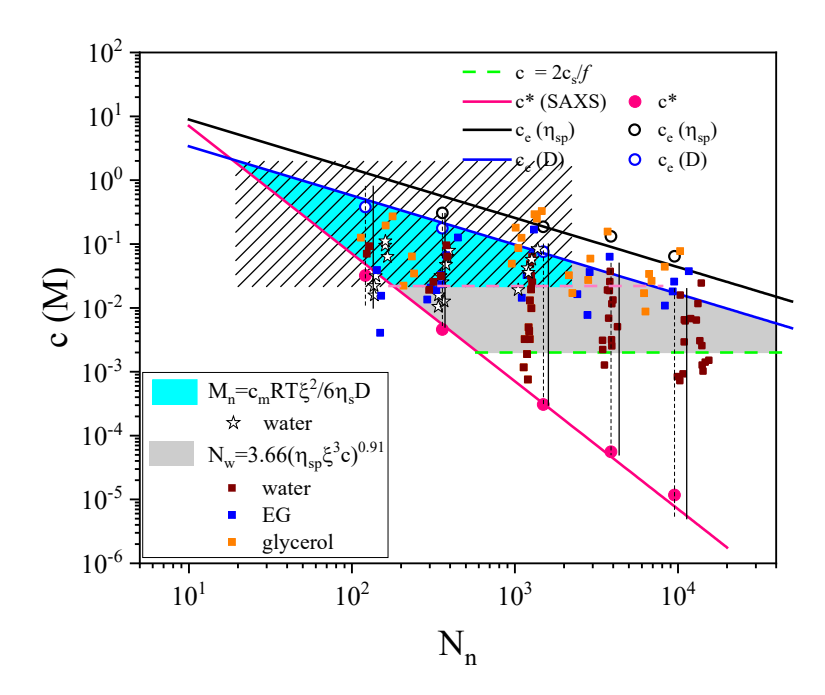


Figure 14. Best methods for determining the molecular weight of polyelectrolytes. The shaded area shows the concentration range over which our methods apply, and this range is enclosed by the entanglement concentration c_e (above) the overlap concentration c^* (below) and a lowest possible concentration that has the same number density of counterions as salt ions ($c = 2c_s/f$, green dashed line). The method $N_w = 3.66(c\eta_{sp}\xi^3)^{0.91}$ is used to determine N_w shown as the filled squares calculated using the reported dispersity of each molecular weight. The blue area indicates the range that $M_n = \frac{c_m RT\xi^2}{6\eta_s D}$ can be used to determine M_n in water (for $N_n < 2000$ and c > 0.022 M, shown as the pink dashed line) with open stars representing the data obtained from measuring D. Solid black lines indicate the expected N_w , and dashed black lines indicate the expected N_n .

ASSOCIATED CONTENTS

Supporting Information

Static light scattering and intrinsic viscosity results of NaPSS in 0.1 M and 0.5 M NaCl. Small-angle X-ray scattering profile of salt-free CsPSS in water solutions. T₁ and T₂ relaxation time

determination for PFG-NMR experiments and the Stejskal-Tanner plots of five molecular weights of CsPSS in water solutions.

AUTHOR INFORMATION

Corresponding Authors

Louis A. Madsen

Department of Chemistry and Macromolecules Innovation Institute, Virginia Tech, Blacksburg, Virginia 24061, United States;

ORCID https://orcid.org/0000-0003-4588-5183

Email <u>lmadsen@vt.edu</u>

Ralph H. Colby

Department of Materials Science and Engineering, Pennsylvania State University, University Park, Pennsylvania 16802, United States;

ORCID https://orcid.org/0000-0002-5492-6189

Email rhc@plmsc.psu.edu

ORCID

Aijie Han https://orcid.org/0000-0002-9309-5912

Daniele Parisi http://orcid.org/0000-0002-1650-8429

Xiuli Li http://orcid.org/0000-0001-6203-4546

ACKNOWLEDGMENTS

This work is funded by the National Science Foundation Chemistry-1904852. We would like to thank Carlos G. Lopez, Andrey Dobrynin and Michael Rubinstein for helpful discussions.

References

- (1) Dobrynin, A. V.; Colby, R. H.; Rubinstein, M. Scaling Theory of Polyelectrolyte Solutions. *Macromolecules* **1995**, *28*, 1859-1871.
- (2) De Gennes, P. G.; Pincus, P.; Velasco, R. M.; Brochard, F. Remarks on Polyelectrolyte Conformation. *J. phys. (Paris)* **1976**, *37*, 1461-1473.
- (3) Colby, R. H. Structure and linear viscoelasticity of flexible polymer solutions: comparison of polyelectrolyte and neutral polymer solutions. *Rheol. Acta* **2010**, *49*, 425-442.
- (4) Rochas, C.; Domard, A.; Rinaudo, M. Aqueous GPC of electrolytes and polyelectrolytes. *Eur. Polym. J.* **1980**, *16*, 135-140.
- (5) Mori, S. Secondary effects in aqueous size exclusion chromatography of sodium poly (styrene sulfonate) compounds. *Anal. Chem.* **1989**, *61*, 530-534.
- (6) Vrij, A.; Overbeek, J. T. G. Scattering of light by charged colloidal particles in salt solutions. *J. Colloid Sci.* **1962**, *17*, 570-588.
- (7) Brüssau, R.; Goetz, N.; Mächtle, W.; Stölting, J. Charakterisierung von Polyacrylatpolumeren / Characterization of Polyacrylate Samples. *Tenside Surfactants Detergents* **1991**, *28*, 396-406.
- (8) Brown, W. Light Scattering: Principles and Development; Oxford University Press, 1996.
- (9) Rubinstein, M.; Colby, R. H. Polymer Physics; Oxford University Press, 2003.
- (10) Alexandrowicz, Z.; Katchalsky, A. Colligative properties of polyelectrolyte solutions in excess of salt. *J. Polym. Sci., Part A: Gen. Pap.* **1963**, *1*, 3231-3260.
- (11) Takahashi, A.; Kato, T.; Nagasawa, M. The Second Virial Coefficient of Polyelectrolytes. *J. Phys. Chem.* **1967**, *71*, 2001-2010.
- (12) Oosawa, F. *Polyelectrolytes*; Marcel Dekker, 1971.
- (13) Einfeldt, L.; Günther, W.; Klemm, D.; Heublein, B. Peracetylated cellulose: end group modification and structural analysis by means of ¹H-NMR spectroscopy. *Cellulose* **2005**, *12*, 15-24.
- (14) Shit, S. C.; Maiti, S. Application of NMR spectroscopy in molecular weight determination of polymers. *Eur. Polym. J.* **1986**, *22*, 1001-1008.
- (15) Wu, J.; Tan, C.; Zhou, X.; Tan, Y.; Yang, P.; Jiang, Y. Molecular weight analysis of water-soluble poly(phenylene)s using MALDI-TOF MS. *J. Polym. Sci., Part A: Polym Chem.* **2017**, *55*, 2537-2543.
- (16) Gruendling, T.; Weidner, S.; Falkenhagen, J.; Barner-Kowollik, C. Mass spectrometry in polymer chemistry: a state-of-the-art up-date. *Polymer Chemistry* **2010**, *1*, 599-617.
- (17) Muthukumar, M. 50th Anniversary Perspective: A Perspective on Polyelectrolyte Solutions. *Macromolecules* **2017**, *50*, 9528-9560.
- (18) Rumyantsev, A. M.; Jackson, N. E.; Pablo, J. J. d. Polyelectrolyte Complex Coacervates: Recent Developments and New Frontiers. *Annual Review of Condensed Matter Physics* **2021**, *12*, 155-176.
- (19) Ylitalo, A. S.; Balzer, C.; Zhang, P.; Wang, Z.-G. Electrostatic Correlations and Temperature-Dependent Dielectric Constant Can Model LCST in Polyelectrolyte Complex Coacervation. *Macromolecules* **2021**, *54*, 11326-11337.

- (20) Sing, C. E.; Perry, S. L. Recent progress in the science of complex coacervation. *Soft Matter* **2020**, *16*, 2885-2914.
- (21) Larson, R. G.; Liu, Y.; Li, H. Linear viscoelasticity and time-temperature-salt and other superpositions in polyelectrolyte coacervates. *Journal of Rheology* **2021**, *65*, 77-102.
- (22) Han, A.; Colby, R. H. Rheology of Entangled Polyelectrolyte Solutions. *Macromolecules* **2021**, *54*, 1375-1387.
- (23) Ferry, J. D. Viscoelastic Properties of Polymers; Wiley, 1970.
- (24) Graessley, W. W. Polymeric Liquids and Networks: Dynamics and Rheology. Garland Science, 2008; pp 721-722.
- (25) Chen, G.; Perazzo, A.; Stone, H. A. Electrostatics, conformation, and rheology of unentangled semidilute polyelectrolyte solutions. *Journal of Rheology* **2021**, *65*, 507-526.
- (26) Matsumoto, A. Rheology of Polyelectrolyte Solutions: Current Understanding and Perspectives. *Nihon Reoroji Gakkaishi* **2022**, *50*, 43-50.
- (27) Ferry, J. D.; Williams, M. L.; Stern, D. M. Slow relaxation mechanisms in concentrated polymer solutions. *The Journal of Physical Chemistry* **1954**, *58*, 987-992.
- (28) Essafi, W.; Spiteri, M.-N.; Williams, C.; Boue, F. Hydrophobic Polyelectrolytes in Better Polar Solvent. Structure and Chain Conformation As Seen by SAXS and SANS. *Macromolecules* **2009**, *42*, 9568-9580.
- (29) Lopez, C. G.; Rogers, S. E.; Colby, R. H.; Graham, P.; Cabral, J. T. Structure of sodium carboxymethyl cellulose aqueous solutions: A SANS and rheology study. *J. Polym. Sci., Part B: Polym Phys* **2015**, *53*, 492-501.
- (30) Essafi, W.; Haboubi, N.; Williams, C.; Boué, F. Weak Temperature Dependence of Structure in Hydrophobic Polyelectrolyte Aqueous Solution (PSSNa): Correlation between Scattering and Viscosity. *J. Phys. Chem. B* **2011**, *115*, 8951-8960.
- (31) Drifford, M.; Dalbiez, J. P. Light scattering by dilute solutions of salt-free polyelectrolytes. *The Journal of Physical Chemistry* **1984**, *88*, 5368-5375.
- (32) Nierlich, M.; Williams, C. E.; Boue, F.; Cotton, J. P.; Daoud, M.; Farnoux, B.; Jannink, G.; Picot, C.; Moan, M.; Wolff, C.; et al. Small-Angle Neutron-Scattering by Semi-Dilute Solutions of Polyelectrolyte. *Journal De Physique* **1979**, *40*, 701-704.
- (33) Kaji, K.; Urakawa, H.; Kanaya, T.; Kitamaru, R. Phase diagram of polyelectrolyte solutions. *Journal de Physique* **1988**, *49*, 993-1000.
- (34) Combet, J.; Lorchat, P.; Rawiso, M. Salt-free aqueous solutions of polyelectrolytes: Small angle X-ray and neutron scattering characterization. *The European Physical Journal Special Topics* **2012**, *213*, 243-265.
- (35) Ermi, B. D.; Amis, E. J. Influence of Backbone Solvation on Small Angle Neutron Scattering from Polyelectrolyte Solutions. *Macromolecules* **1997**, *30*, 6937-6942.
- (36) Sharratt, W. N.; O'Connell, R.; Rogers, S. E.; Lopez, C. G.; Cabral, J. T. Conformation and Phase Behavior of Sodium Carboxymethyl Cellulose in the Presence of Mono- and Divalent Salts. *Macromolecules* **2020**, *53*, 1451-1463.
- (37) Boris, D. C.; Colby, R. H. Rheology of Sulfonated Polystyrene Solutions. *Macromolecules* **1998**, *31*, 5746-5755.
- (38) Krause, W. E.; Tan, J. S.; Colby, R. H. Semidilute solution rheology of polyelectrolytes with no added salt. *J. Polym. Sci., Part B: Polym Phys* **1999**, *37*, 3429-3437.

- (39) Dou, S.; Colby, R. H. Solution Rheology of a Strongly Charged Polyelectrolyte in Good Solvent. *Macromolecules* **2008**, *41*, 6505-6510.
- (40) Doi, M.; Doi, P. A. P. M.; Edwards, S. F. The Theory of Polymer Dynamics; Clarendon Press, 1986.
- (41) Förster, S.; Schmidt, M.; Antonietti, M. Static and dynamic light scattering by aqueous polyelectrolyte solutions: effect of molecular weight, charge density and added salt. *Polymer* **1990**, *31*, 781-792.
- (42) Koene, R. S.; Nicolai, T.; Mandel, M. Scaling relations for aqueous polyelectrolyte-salt solutions. 2. Quasi-elastic light scattering as a function of polyelectrolyte concentration and salt concentration. *Macromolecules* **1983**, *16*, 227-231.
- (43) Förster, S.; Schmidt, M. Polyelectrolytes in solution. In *Physical Properties of Polymers*, Springer Berlin Heidelberg, 1995; pp 51-133.
- (44) Oostwal, M. G.; Blees, M. H.; De Bleijser, J.; Leyte, J. C. Chain self-diffusion in aqueous salt-free solutions of sodium poly(styrenesulfonate). *Macromolecules* **1993**, *26*, 7300-7308.
- (45) Hirose, E.; Iwamoto, Y.; Norisuye, T. Chain Stiffness and Excluded-Volume Effects in Sodium Poly(styrenesulfonate) Solutions at High Ionic Strength. *Macromolecules* **1999**, *32*, 8629-8634.
- (46) Yashiro, J.; Norisuye, T. Excluded-volume effects on the chain dimensions and transport coefficients of sodium poly(styrene sulfonate) in aqueous sodium chloride. *J. Polym. Sci., Part B: Polym Phys* **2002**, 40, 2728-2735.
- (47) Callaghan, P. T. Translational Dynamics and Magnetic Resonance: Principles of Pulsed Gradient Spin Echo NMR; Oxford University Press, 2011.
- (48) Drifford, M.; Dalbiez, J. P. Light scattering by dilute solutions of salt-free polyelectrolytes. *J. Phys. Chem.* **1984**, *88*, 5368-5375.
- (49) Cohen, J.; Priel, Z.; Rabin, Y. Viscosity of dilute polyelectrolyte solutions. J. Chem. Phys. 1988, 88, 7111-7116.
- (50) Chen, S.-P.; Archer, L. A. Relaxation dynamics of salt-free polyelectrolyte solutions using flow birefringence and rheometry. *J. Polym. Sci., Part B: Polym Phys* **1999**, *37*, 825-835.
- (51) Prini, R. F.; Lagos, A. E. Tracer diffusion, electrical conductivity, and viscosity of aqueous solutions of polystyrenesulfonates. *J. Polym. Sci., Part A: Gen. Pap.* **1964**, *2*, 2917-2928.
- (52) Oostwal, M.; Odijk, T. Novel dynamic scaling hypothesis for semidilute and concentrated solutions of polymers and polyelectrolytes. *Macromolecules* **1993**, *26*, 6489-6497.
- (53) Üzüm, C.; Christau, S.; von Klitzing, R. Structuring of Polyelectrolyte (NaPSS) Solutions in Bulk and under Confinement as a Function of Concentration and Molecular Weight. *Macromolecules* **2011**, *44*, 7782-7791.
- (54) Lopez, C. G. Scaling and Entanglement Properties of Neutral and Sulfonated Polystyrene. *Macromolecules* **2019**, *52*, 9409-9415.
- (55) Lopez, C. G.; Linders, J.; Mayer, C.; Richtering, W. Diffusion and viscosity of unentangled polyelectrolytes. *Macromolecules* **2021**, *54*, 8088-8103.
- (56) Daoud, M.; Cotton, J. P.; Farnoux, B.; Jannink, G.; Sarma, G.; Benoit, H.; Duplessix, C.; Picot, C.; de Gennes, P. G. Solutions of Flexible Polymers. Neutron Experiments and Interpretation. *Macromolecules* **1975**, *8*, 804-818.
- (57) Dobrynin, A. V.; Rubinstein, M. Theory of polyelectrolytes in solutions and at surfaces. *Prog. Polym. Sci.* **2005**, *30*, 1049-1118.

- (58) Colby, R. H.; Boris, D. C.; Krause, W. E.; Tan, J. S. Polyelectrolyte conductivity. *J. Polym. Sci., Part B: Polym Phys* **1997**, *35*, 2951-2960.
- (59) Stejskal, E. O.; Tanner, J. E. Spin Diffusion Measurements: Spin Echoes in the Presence of a Time-Dependent Field Gradient. *J. Chem. Phys.* **1965**, *42*, 288-292.
- (60) Carrazzone, R. J.; Li, X.; Foster, J. C.; Uppala, V. V. S.; Wall, C. E.; Esker, A. R.; Madsen, L. A.; Matson, J. B. Strong Variation of Micelle-Unimer Coexistence as a Function of Core Chain Mobility. *Macromolecules* **2021**, *54*, 6975-6981.
- (61) Callaghan, P. T.; Pinder, D. N. A pulsed field gradient NMR study of self-diffusion in a polydisperse polymer system: dextran in water. *Macromolecules* **1983**, *16*, 968-973.
- (62) Chen, A.; Wu, D.; Johnson, C. S. Determination of Molecular Weight Distributions for Polymers by Diffusion-Ordered NMR. *Journal of the American Chemical Society* **1995**, *117*, 7965-7970.
- (63) Meerwall, E. v.; Ozisik, R.; Mattice, W. L.; Pfister, P. M. Self-diffusion of linear and cyclic alkanes, measured with pulsed-gradient spin-echo nuclear magnetic resonance. *The Journal of Chemical Physics* **2003**, *118*, 3867-3873.